

PHOTODISINTEGRATION OF HELIUM. II

A. N. GORBUNOV and V. M. SPIRIDONOV

P. N. Lebedev Physical Institute, Academy of Sciences, U.S.S.R.

Submitted to JETP editor December 14, 1957

J. Exptl. Theoret. Phys. (U.S.S.R.) **34**, 862-865 (April, 1958)

The $\text{He}^4(\gamma, n)\text{He}^3$ reaction was investigated using a Wilson chamber. The method for treating the He^3 track data is described. The dependence of the reaction cross section on γ -ray energy and the angular distributions of the reaction products were measured. σ_{int} and $\sigma_{\text{b}} = \int \sigma(W) W^{-1} dW$ are computed from the curve for $\sigma(W)$.

1. INTRODUCTION

IN the first part of this work^{1,*} we gave a detailed description of experiments on photodisintegration of helium using a Wilson chamber in a magnetic field, placed in the beam of the synchrotron of the Physical Institute of the Academy of Sciences, which gives a maximum energy of 170 Mev. We also gave the results of a study of the $\text{He}^4(\gamma, p)\text{H}^3$ reaction from the analysis of 9000 cloud chamber pictures, including the energy distributions of the protons and tritons and the energy dependence of the cross section for the reaction.

We shall here describe the results of investigation of the $\text{He}^4(\gamma, n)\text{He}^3$ from processing of the same photographs.

2. PROCESSING OF PHOTOGRAPHS

As was mentioned in I, the $\text{He}^4(\gamma, n)\text{He}^3$ reaction is characterized by the emission of a single charged particle, the He^3 recoil nucleus, which gives a high density track in the cloud chamber (Fig. 1). A single charged particle with a high density track can also occur from (γ, n) reactions on C and O nuclei, which are contained in the vapor in the cloud chamber. However the mean length of these tracks is 4–5 mm, and their maximum does not exceed 15 mm, so they can be assigned to events in helium only for photon energies between 20.6 (the threshold for the $\text{He}^4(\gamma, n)\text{He}^3$ reaction) and 25 Mev. In investigating the energy dependence of the cross section for the $\text{He}^4(\gamma, n)\text{He}^3$ reaction, we therefore restricted ourselves to the range of photon energies $h\nu \geq 27$ Mev, in which the (γ, n) reaction could be reliably identified.

Since there are only two particles in the final

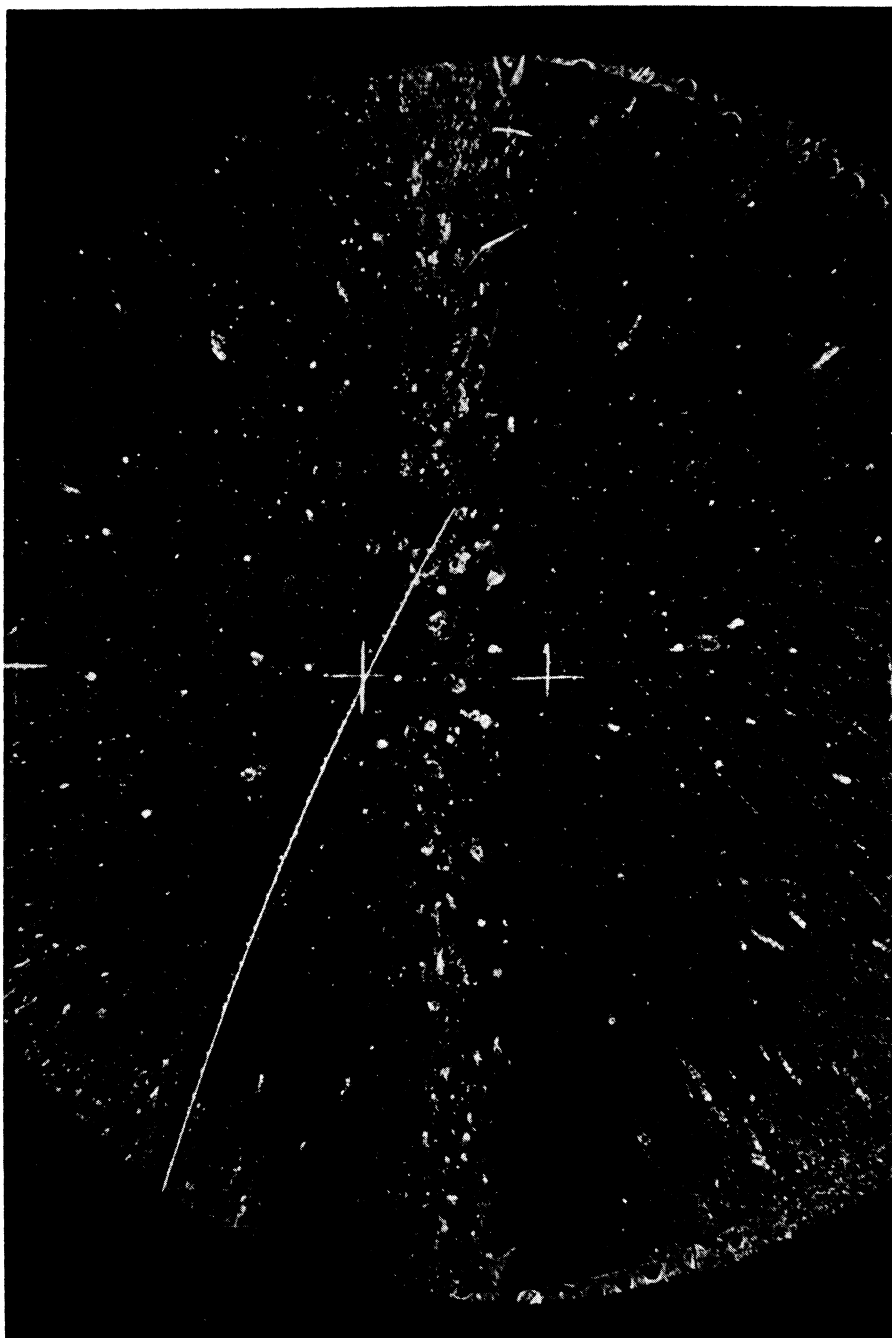
state for the $\text{He}^4(\gamma, n)\text{He}^3$ reaction, we can, as in the $\text{He}^4(\gamma, p)\text{H}^3$ reaction, use the conservation laws to determine the energy of the photon which produced the reaction, from a knowledge of the angle of emergence and the momentum of one of the particles (the He^3 nucleus). For the measurement of angles of emergence and momenta of He^3 nuclei, we selected from all the recorded cases of the $\text{He}^4(\gamma, n)\text{He}^3$ reaction those He^3 tracks which had a sufficient projected length (≥ 53 mm) on the bottom plane of the chamber, and the momenta were determined from the curvature of the tracks in the magnetic field.

The procedure for measuring angles and momenta, as well as the necessary corrections, were described in I. Here we need only add that, since for low energy He^3 nuclei the curvature changed along the track, the measurement gave some average value of the momentum, and a suitable correction was made graphically to find the true momentum. However, if we limited ourselves to only those He^3 tracks which had a large projected length, we would impose a strong limitation on the energy range of the photons for which we could get the energy dependence of the cross section. Actually, if for example the He^3 nucleus is emitted at an angle of 180° to the γ -ray direction and has a range of 5.3 cm in the chamber gas, the energy of the photon responsible for this event is ~ 40 Mev, and this limiting energy depends essentially on the angle of emergence of the He^3 nucleus. Because of this, we also processed short tracks of He^3 nuclei stopping in the chamber gas. For these the path length and spatial angles were measured with a special stereocomparator.* In this case the momenta of the He^3 nuclei were found from the range-

*The stereocomparator was developed in the cosmic ray laboratory of the Physical Institute of the Academy of Sciences by engineer A. G. Novikov.

*This paper will be cited as I.

FIG. 1. $\text{He}^4(\gamma, n)\text{He}^3$ reaction.
The single dense track is a He^3 nucleus.



momentum relation calculated for the mixture of gases in the chamber.

Of the total number of 2685 cases of the $\text{He}^4(\gamma, n)\text{He}^3$ reaction recorded, 722 tracks of He^3 nuclei were analyzed. As in our study of the $\text{He}^4(\gamma, p)\text{H}^3$ reaction, all the measured He^3 tracks were incorporated in a nomogram which served as the primary material for further computations of energy dependence and angular distributions.

3. RESULTS

A. Dependence of the Cross Section for the $\text{He}^4(\gamma, n)\text{He}^3$ Reaction on Photon Energy

The dependence of the cross section for the (γ, n) reaction on photon energy is given in Fig. 2. For the reasons given above, it was not drawn from the reaction threshold (20.6 Mev), but from 27 Mev.

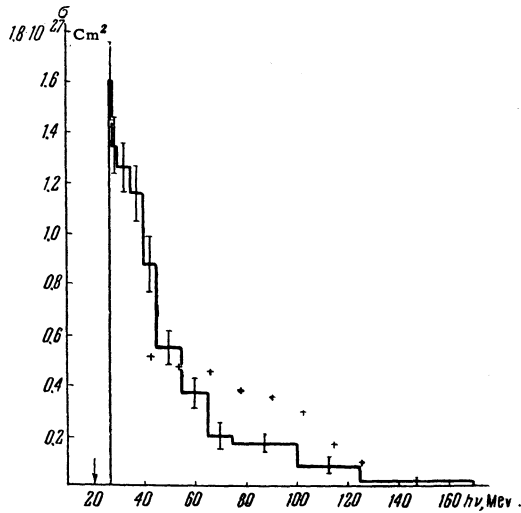


FIG. 2. Dependence of the cross section for the $\text{He}^4(\gamma, n)\text{He}^3$ reaction on photon energy. Only statistical errors are shown on the figure. The reaction threshold (20.6 Mev) is indicated by the arrow. The points marked with a + are the data of Ref. 2.

As we see from the figure, the (γ, n) reaction on helium has resonant character, with a maximum of $\sim 1.6 \times 10^{-21} \text{ cm}^2$ at an energy of 27–28 Mev. The position and height of the maximum agree within the limits of error with the corresponding values for the (γ, p) reaction.

Comparison of the curves for the cross sections for the (γ, p) and (γ, n) reactions shows that they have the same shape, although the curve for the (γ, n) reaction runs a little higher for photon energies above 35 Mev. This difference is possibly due to the large corrections made to the measured values of the momenta of He^3 nuclei, of which we spoke before, and also to neglect of multiple scattering. Whether this difference is real will be settled in experiments which are now being done with a magnetic field of twice the intensity and a lower pressure of the gas mixture in the cloud chamber.

In Fig. 2 we include for comparison the results of measurements of the cross section for the (γ, n) reaction on helium which were found in Ref. 2 using thick-layered emulsions. As we see from Fig. 2, these results agree with our data only at ~ 55 Mev, while for higher energies they give cross sections which are approximately twice as large.

TABLE I*

Photon energy E_γ , Mev	$\sigma_{\text{int}} = \int_{20.6}^{E_\gamma} \sigma(W) dW$, Mev-millibarns
40	21.6 ± 0.9
100	41.3 ± 1.7
170	43.8 ± 1.8

*Only statistical errors are given.

From the cross section curve for the (γ, n) reaction, we calculated the integral cross section $\sigma_{\text{int}} = \int \sigma(W) dW$ (Table I), and the quantity $\sigma_b = \int_{20.6}^{170} \sigma(W) W^{-1} dW = (1.09 \pm 0.08)$ millibarns.

The value of σ_b agrees exactly with the value of σ_b found in I for the (γ, p) reaction. The values of the integral cross section for the (γ, n) reaction at 100 and 170 Mev are somewhat greater than the corresponding values for the (γ, p) reaction.

B. Angular Distributions

The angular distributions (in the center-of-mass system, c.m.s.) of the neutrons from the $\text{He}^4(\gamma, n)\text{He}^3$ reaction are given in Fig. 3 for two

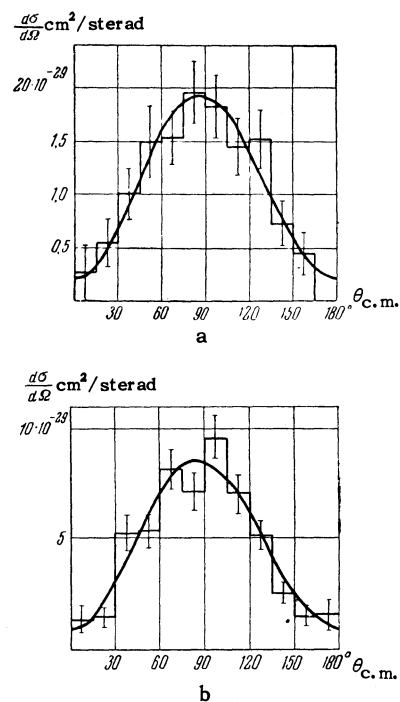


FIG. 3. Angular distributions in the c.m.s. of neutrons from the $\text{He}^4(\gamma, n)\text{He}^3$ reaction with photons of energy: a) 27–30; b) 30–170 Mev.

photon energy ranges: 27–30 Mev and 30–170 Mev. They were obtained by reflecting the angular distributions of the He^3 nuclei about 90° in the c.m.s. These energy ranges were chosen for convenience of comparison with the angular distributions of protons from the (γ, p) reaction on helium, which were given in I.

The angular distributions were approximated by curves of the form

$$A(\sin^2 \theta + \beta \sin^2 \theta \cos \theta + \delta).$$

The values of the coefficients A , β , δ were

fitted by a least squares method, and are given in Table II.

TABLE II

Photon energy E_γ , Mev	$A \cdot 10^{29}$ $\text{cm}^2/\text{sterad}$	β	δ
27—30	1.7 ± 0.2	0.11 ± 0.18	0.12 ± 0.07
30—170	7.5 ± 0.6	0.17 ± 0.13	0.12 ± 0.07

From Figure 3 and Table II we see that, in going from photon energies below 30 Mev to energies greater than 30 Mev, the angular distribution of the neutrons remains unchanged within the limits of error of the experiment, and is close to a $\sin^2 \theta$ distribution in the c.m.s. On the other hand, as was shown in I, the asymmetry of the angular distribution of the protons from the (γ, p) reaction on helium changes markedly in the photon energy region 30 — 35 Mev, so that in the 30 — 170 Mev range the maximum of the angular distribution in the c.m.s. shifts forward to an angle of 65 — 70°.

It is interesting to note that similar results are found for the angular distributions of photoprotons from more complex nuclei (C, Al, Ni, Mo). In fact³⁻⁶ the angular distributions of the photoprotons have their maximum at an angle of 60 — 70° and contain an appreciable isotropic part. At the same time, the angular distributions of the photoneutrons³ are well described by curves of the form $a + b \sin^2 \theta$, symmetric around 90°. Thus if we disregard the appreciable isotropic part of these distributions (which may be due to evaporation processes and also to internal scattering of the particles inside the nucleus), there is a qualitative similarity of these results to the curves obtained for helium.

These features of the angular distributions of protons and neutrons can be explained from the point of view of a model of direct absorption of the photon by an individual nucleon, as proposed by Courant,⁷ supplemented by including electric quadrupole absorption of the photons. Actually, from the point of view of this model, at low energies there is electric dipole absorption, so that the angular distributions of protons and neutrons have the form $\sin^2 \theta$. At energies greater than

30 Mev, electric quadrupole absorption begins to appear, which because of interference with the dipole absorption results in a shift of the maximum of the proton angular distribution toward smaller angles. However, the electric quadrupole absorption does not contribute to the neutron yield since the effective charge of the neutron is in this case equal to zero. Thus the angular distribution of the neutrons remains close to $\sin^2 \theta$ even at high energies.

The quasideuteron model of photon absorption, proposed in papers of Khokhlov⁸ and Levinger⁹ cannot be responsible for the observed effects, since for photon energies greater than 30 Mev it would give an angular distribution of the neutrons similar to that for the protons, but with the maximum shifted in the reverse direction.

In conclusion, the authors express their gratitude to Prof. P. A. Cerenkov for continual interest in the work, to Iu. K. Khokhlov, V. V. Daragan and Iu. M. Shirokov for discussion of the results, to A. G. Gerasimov, V. S. Silaev, N. N. Novikov, K. V. Chekhovich and Hu Cheng-Yü for participating in the analysis of photographs, and to the operating group of the synchrotron.

¹A. N. Gorbunov and V. M. Spiridonov, J. Exptl. Theoret. Phys. (U.S.S.R.) **33**, 21 (1957); Soviet Phys. JETP **6**, 16 (1958).

²G. De Saussure and L. S. Osborne, Phys. Rev. **99**, 843 (1955).

³S. A. E. Johansson, Phys. Rev. **97**, 434 (1955).

⁴I. V. Chuvilo and V. G. Shevchenko, J. Exptl. Theoret. Phys. (U.S.S.R.) **32**, 1335 (1957); Soviet Phys. JETP **5**, 1090 (1957).

⁵Mann, Halpern and Rothman, Phys. Rev. **87**, 146 (1952).

⁶H. Hendel, Z. f. Physik **135**, 168 (1953).

⁷E. D. Courant, Phys. Rev. **82**, 703 (1951).

⁸Iu. K. Khokhlov, J. Exptl. Theoret. Phys. (U.S.S.R.) **23**, 241 (1952).

⁹J. S. Levinger, Phys. Rev. **84**, 43 (1951).